Available online at www.sciencedirect.com
ScienceDirect
Bioorganic & Medicinal Chemistry 14 (2006) 8352–8358
Bioorganic & Medicinal Chemistry

Synthesis and biological evaluation of a cyclic ether fluorinated noscapine analog

Ritu Aneja,* Surya N. Vangapandu and Harish C. Joshi

Laboratory for Drug Discovery and Research, Department of Cell Biology, Emory University School of Medicine, 615 Michael Street, Atlanta, GA 30322, USA

Received 11 July 2006; accepted 7 September 2006
Available online 27 September 2006

Abstract—We present here a novel semi-synthetic cyclic ether fluorinated noscapine analog (CEFNA) that shows potent antiproliferative and anticancer activity in both hormone-responsive (MCF-7) and hormone non-responsive (MDA-MB-231) breast cancer cells. Interestingly, it is also effective against MCF-7/Adr, an adriamycin-resistant variant of MCF-7 cells. Immunofluorescence experiments showed numerous micronuclei, indicative of apoptotic cell death triggered by this novel analog. Mechanistically, CEFNA exerts a strong antimitotic effect as revealed by cell-cycle studies that show a dose-dependent increase in G2/M population preceding a rising sub-G1 population, suggesting apoptosis.

1. Introduction

Although the effectiveness of microtubule-targeting drugs has been validated by the extensive use of several vinca alkaloids and taxanes for the treatment of a wide variety of human cancers, their clinical success has been limited by the emergence of drug-resistance[1–3] and associated toxicities such as leucocytopenias, diarrhea, alopecia, and peripheral neuropathies due to the blockage of axonal transport.[4–6] This has driven an ongoing search for novel microtubule-targeting compounds that display favorable toxicity profiles, have better therapeutic indices and improved pharmacological characteristics.

Our laboratory recently discovered the previously unknown tubulin-binding and anticancer property of an antitussive phthalideisoquinoline alkaloid, noscapine.[7] To enhance its activity, our efforts have been focused on rational drug design and synthesis leading to an array of noscapinoids, which are at different stages of chemical and biological characterization. Some of them have been shown to suppress the dynamics of microtubule assembly and block cell-cycle progression at mitosis, followed by apoptotic cell death in a wide variety of cancer cell types.[8–16]

Here, we describe a selective and high-yield scheme for the synthesis of a cyclic ether fluorinated noscapine analog (CEFNA) and an evaluation of its anticancer activity. Our results show that CEFNA significantly inhibited proliferation of human breast adenocarcinoma cells (estrogen- and progesterone-receptor positive, MCF-7 and estrogen- and progesterone-receptor negative, MDA-MB-231) irrespective of their hormone status. Surprisingly, CEFNA showed a ~6-fold lower IC_{50} in MCF-7 cells as compared to the parent compound, noscapine.[9] Even the hormone-refractory MDA-MB-231 cells respond with a ~7-fold lower IC_{50} value when compared to noscapine.[9] This inhibition of cellular proliferation correlated with the appearance of numerous fragmented nuclei at 72 h of drug exposure as shown by DAPI staining. Immunofluorescence studies using confocal microscopy revealed that this fluorinated cyclic ether noscapine analog affects spindle architecture. Numerous mitotically arrested figures were evident at 12–24 h of drug treatment. This was followed by the emergence of multilobed nuclei at 48 h suggesting multiple rounds of DNA synthesis due to abrogated checkpoint mechanisms. At 72 h, micronuclei reminiscent of apoptotic bodies were visible, suggestive apoptosis triggered perhaps due to genotoxic stress subsequent to overaccumulation of

Keywords: Noscapine; Fluorination; Cyclic ethers; Anticancer.
* Corresponding author. Tel.: +1 404 727 0445; fax: +1 404 727 6256; e-mail: raneja@emory.edu

0968-0896/$ - see front matter © 2006 Elsevier Ltd. All rights reserved.
doi:10.1016/j.bmc.2006.09.012

DNA. Cell-cycle progression studies revealed a G2/M arrest followed by the appearance of a substantial hypodiploid sub-G1 population that indicates fragmented DNA, characteristic of apoptosis.

2. Results and discussion

2.1. Chemistry

Our lead compound, noscapine, comprises of isoquinoline and benzofuranone ring systems joined by a labile C–C chiral bond and both these ring systems contain several vulnerable methoxy groups. Thus, achieving selective halogenation at C-9 position without disruption and cleavage of these labile groups and C–C bonds was challenging. After careful titration of many conditions, we have been successful in developing simple, selective, efficient, and reproducible synthetic procedures to achieve halogenation at C-9 position. The synthetic route for the preparation of the cyclic ether fluorinated noscapine analogs (CEFNA, **4**) is discussed below.

First, the synthesis of cyclic ether analog of noscapine **2** that is required as an intermediate in the preparation of compound **4** was achieved by using a previously described procedure.[17] Briefly, compound **2** was prepared by adding a solution of noscapine in boron trifluoride dietherate dropwise at 0 °C to a solution of sodium borohydride in dry THF. The mixture was stirred at 0 °C for 1 h and then refluxed for another 2 h to afford the desired reduced noscapine (**2**) as a thick yellow oil in 95% yield.

Next, we carried out bromination of the cyclic ether noscapine analog **2** using bromine water in the presence of HBr (Scheme 1) as described previously with minor modifications.[12,18] The cyclic ether noscapine analog **2** was dissolved in minimum amount of 48% hydrobromic acid with continuous stirring followed by the addition of freshly prepared bromine water over a period of 1 h untill the appearance of an orange precipitate. The reaction mixture was then stirred at room temperature for 1 h to attain completion. The pH of the resultant mixture was adjusted to 10 using ammonia solution to obtain the cyclic ether brominated noscapine analog **3** in 80% yield. Excess amount of HBr or longer reaction times were avoided since they resulted into the hydrolyzed products, meconine and cotarnine. The bromination took place selectively on ring A of isoquinoline nucleus at position C-9 and was confirmed by an absence of C-9 aromatic proton at δ 6.30 ppm in the ^{1}H NMR spectrum of the product. ^{13}C NMR and HRMS data further supported the structure of the compound.

Aromatic fluorination of cyclic ether brominated noscapine analog **3** was achieved using Br/F exchange reaction by employing the fluoride form of Amberlyst-A 26, a macroreticular anion-exchange resin containing quaternary ammonium groups. The method described[19] for Hal/F exchange may also be applied to other Hal/Hal′ exchange reactions. In Br/F exchange reactions, good yields were obtained only when a large molar ratio of the resin with respect to the substrate was employed. Thus, after refluxing a solution of reduced bromonoscapine in anhydrous THF and an excess of Amberlyst-A 26 (fluorine, polymer-supported, 10 mequiv of dry resin; the average capacity of the resin is 4 mequiv/g) for 12 h, the resin was filtered off and the solvent was removed in vacuo to afford the desired compound **4** in 72% yield. The resin was recovered by washing with 1 N NaOH and then rinsing thoroughly with water until neutrality to generate the hydroxy-form of the resin. It was then stirred overnight with 1 N aqueous hydrofluoric acid, washed with acetone, ether, and dried in a vacuum oven at 50 °C for 12 h to afford the regenerated Amberlyst-A 26 (fluorine, polymer-supported), which can be reused.

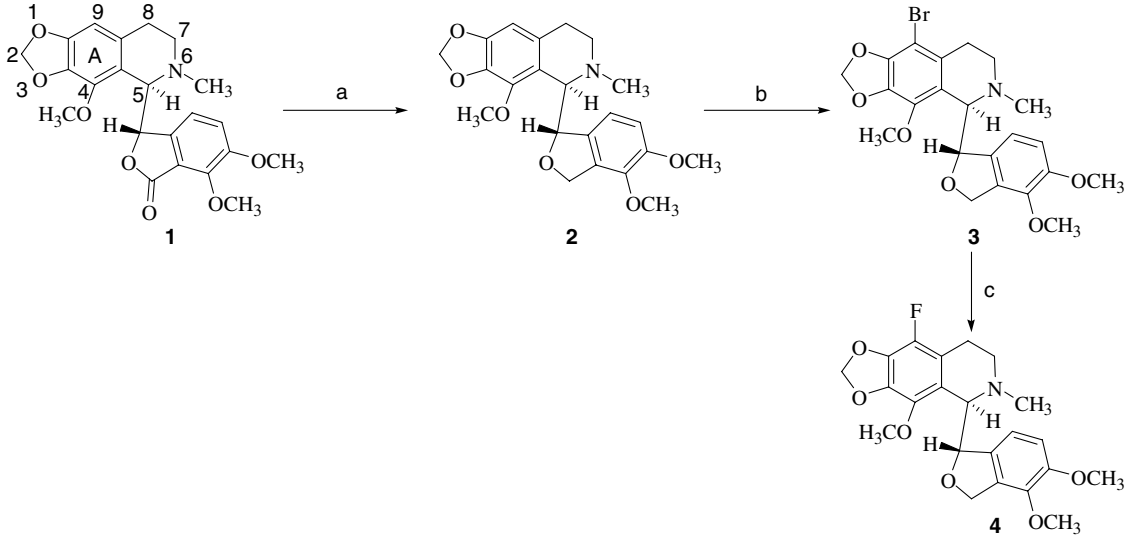

Scheme 1. Synthesis of cyclic ether fluorinated noscapine analog (CEFNA). Reagents and conditions: (a) $NaBH_4/BF_3$. Et_2O, THF, 95%; (b) Br_2-H_2O, 48% HBr, 80%; (c) F_2, Amberlyst-A, THF, 72%.

2.2. Biology

2.2.1. CEFNA inhibits proliferation of human cancer cells. We have previously shown that noscapinoids are potent antitumor agents that target microtubules.[7–16,20] Since multidrug resistance is a serious limitation of the existing chemotherapeutic drugs, we first examined the effect of CEFNA on the proliferation of MCF-7/Adr breast cancer cells, which are derived from the MCF-7 cell line and exhibit multidrug resistance due to overexpression of the drug pump P-glycoprotein.[21] The IC_{50} value of CEFNA was 6.9 and 6.2 μM, respectively, in MCF-7/Adr and the parent MCF-7 cells (Fig. 1A). The quite similar sensitivity of the adriamycin-resistant cells thus suggests that CEFNA is a rather weak substrate for P-glycoprotein, that pumps the drug out thereby reducing the intracellular accumulation of the drug. On the other hand, MCF-7/Adr cells are resistant to paclitaxel and this is not unexpected as paclitaxel is a substrate of pgp.[22] We next moved onto test the efficacy of CEFNA to inhibit proliferation of MDA-MB-231 cells that are hormone non-responsive. The IC_{50} was found to be 5.7 μM (Fig. 1A). This was even lower than the IC_{50} observed for MCF-7 and MCF-7/Adr cells. Figure 1B shows a typical visualization of MDA-MB-231 cells treated with 25 μM CEFNA for 48 h. DMSO controls exhibit normal intact cellular morphology, whereas CEFNA treatment clearly shows dying cells. The loss of membrane integrity in dead and dying cells allows the preferential uptake of labels like trypan blue. The blue dead cells due to trypan blue uptake were counted using a hemocytometer and the percentage of live/dead cells upon CEFNA exposure for different incubation times is depicted in Figure 1C. We further investigated this morphological evaluation by DAPI staining of MDA-MB-231 cells treated with 25 μM CEFNA for 72 h and observed condensed chromatin along with numerous fragmented nuclei (shown by white arrowheads), indicative of apoptotic cell death (Fig. 2).

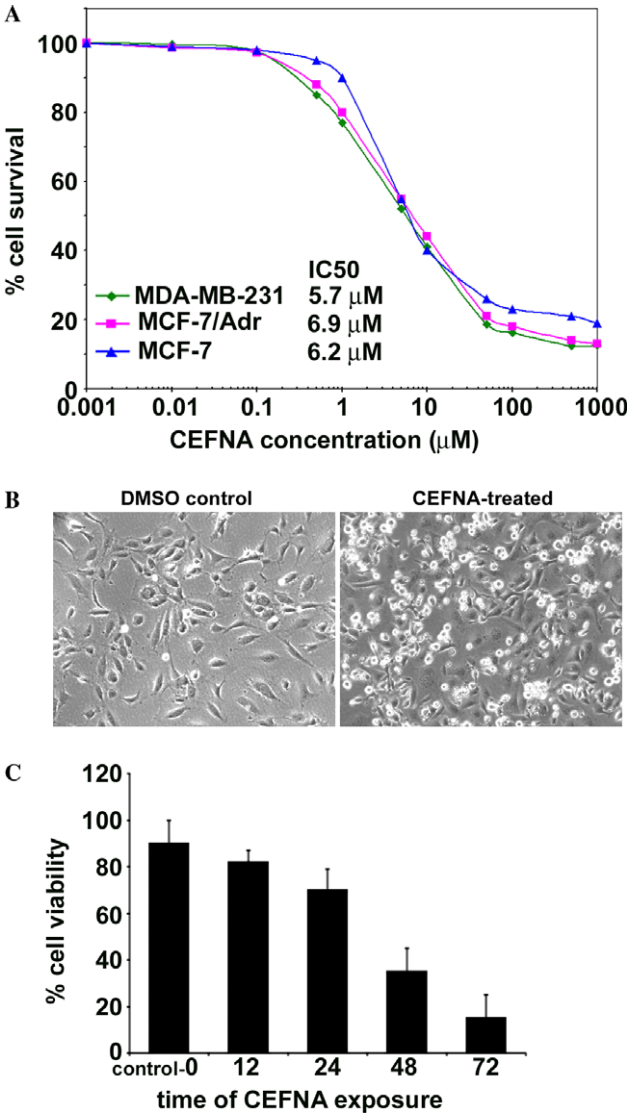

Figure 1. CEFNA actively inhibits the proliferation of human breast cancer cells. Cells (MCF-7, MCF-7/Adr, and MDA-MB-231) were treated with CEFNA at increasing gradient concentrations for 72 h. The IC_{50} values, which stand for the drug concentration needed to prevent cell proliferation by 50%, were then measured using an in vitro sulforhodamine B assay. Panel A is a plot of percent cell survival versus CEFNA concentrations used for the determination of IC_{50} values. Each value represents the average of three independent experiments performed in triplicate. Panel B is a visualization of control MDA-MB-231 cells (left panel) and cells treated with 25 μM CEFNA for 48 h. Panel C is a quantitative bar-graphical representation showing percent cell viability upon 25 μM CEFNA administration for the noted hours measured using trypan blue-based exclusion assay.

2.2.2. CEFNA affects spindle architecture. Using immunofluorescence microscopy, we then examined the spindle architecture of cells treated with 25 μM CEFNA. Whereas untreated cells exhibited normal radial microtubule arrays, cells treated with CEFNA for 24 h showed pronounced multipolar spindles and condensed chromosomes indicating mitotic arrest (Fig. 3). These mitotic figures begin to appear as early as 12 h of CEFNA treatment. This was probably due to the activation of the spindle assembly checkpoint, a cellular surveillance mechanism that monitors the integrity of the mitotic spindle.[23] After 48 h of treatment, large multilobed nuclei (multinucleation) was evident that suggested multiple rounds of DNA synthesis. CEFNA-treated MCF-7 cells eventually died probably through the initiation of apoptosis as fragmented micronuclei and apoptotic bodies were observable at 72 h of CEFNA treatment.

2.2.3. CEFNA perturbs cell-cycle progression. We next sought to investigate the precise mechanisms of CEFNA induced cell death. We examined the cell-cycle progression profile of MCF-7 cells treated with CEFNA at three different doses (5, 10, and 25 μM) using fluorescence activated cell sorting (FACS) analysis of DNA content (Fig. 4A–C). Fluorescently labeled DNA is a good indicator of cell-cycle progression and cell death. An unreplicated complement of 2N DNA cells represents the G0/G1 phase while duplicated 4N DNA cells represent G2 and M phases. Cells in the process of DNA duplication between 2N and 4N peaks represent S phase when DNA is being synthesized. Less than 2N DNA appears in populations of dying cells that degrade

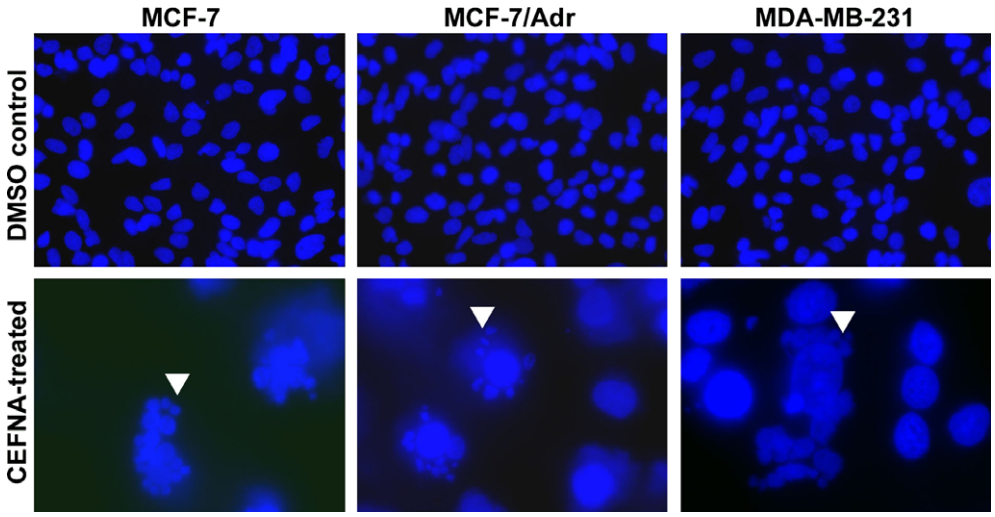

Figure 2. Morphologic criteria for apoptotic cell death include, for example, chromatin condensation with aggregation along the nuclear envelope and plasma membrane blebbing followed by separation into small, apoptotic bodies. Panels show morphological evaluation of nuclei stained with DAPI from control cells (upper panels) and cells treated with 25 μM CEFNA for 72 h (lower panels) using fluorescence microscopy. Several typical features of apoptotic cells such as condensed chromosomes, numerous fragmented micronuclei, and apoptotic bodies are evident (indicated by white arrowheads) upon 72 h of drug treatment.

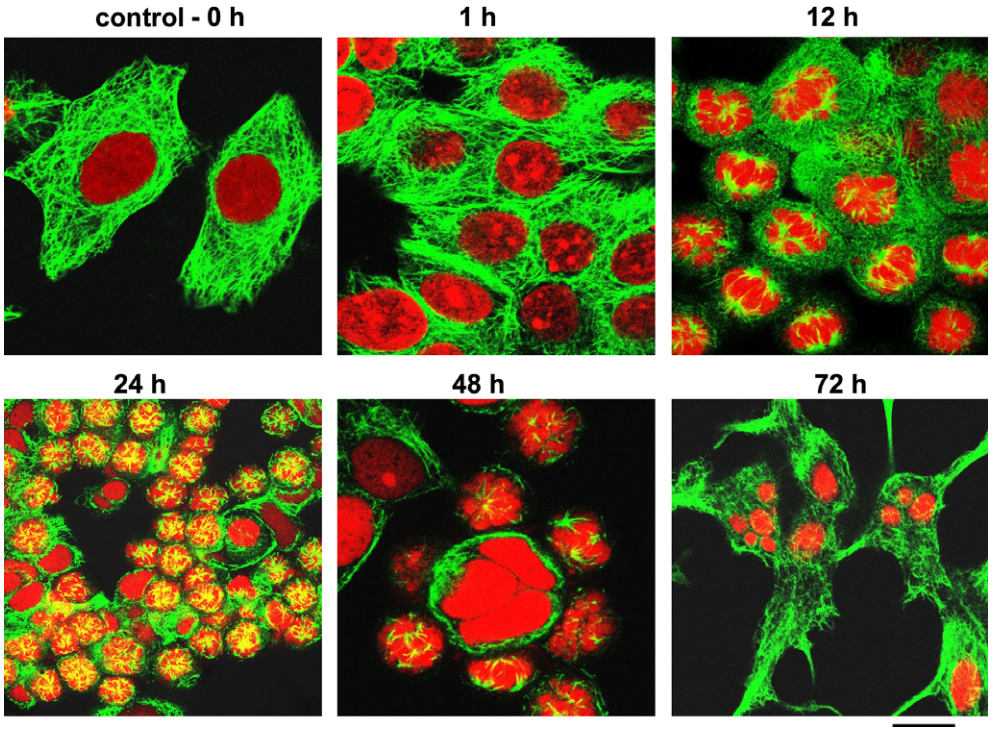

Figure 3. CEFNA induces spindle abnormalities. Panels show immunofluorescence confocal micrographs of MCF-7 cells treated for 0, 1, 12, 24, 48, and 72 h with 25 μM CEFNA. Mitotic figures are abundant at 24 h while apoptotic figures start to appear at 48 h. (Scale bar = 30 μm).

their DNA to different extents. Untreated cells (0 h treatment) showed a typical normal distribution of cell populations in G0/G1 with 2N (unduplicated) DNA content and in G2/M with 4N (duplicated) DNA content. Figure 4A–C represents the cell-cycle progression profile of MCF-7 cells upon CEFNA treatment at different times in a three-dimensional disposition. Treatment of MCF-7 cells with CEFNA for 0, 24, 48, and 72 h led to profound perturbations of the cell cycle (Fig. 4D). Our results show that CEFNA induced a massive accumulation of cells in the G2/M phase at 24 h in a dose-dependent manner. For example, the G2/M cell population increases from 24% in the control to 47% in MCF-7 cells treated with 25 μM CEFNA for 24 h (Fig. 4D). Subsequent to the G2/M block, a characteristic hypodiploid DNA content peak (sub-G1) is seen to be rising at 48 and 72 h of CEFNA treatment for all the three doses studied (Fig. 4D). The progressive gener-

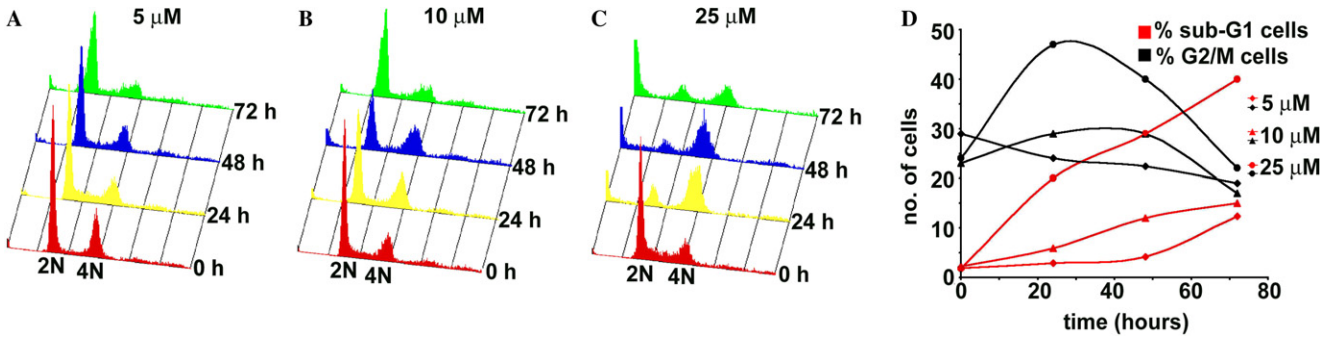

Figure 4. CEFNA inhibit cell-cycle progression at mitosis followed by the appearance of a characteristic hypodiploid (sub-G1) DNA peak, indicative of apoptosis. Panels A–C depict analyses of cell-cycle distribution in a three-dimensional disposition as determined by flow cytometry in MCF-7 cells treated with 5, 10, and 25 μM CEFNA. Panel D is a graphical representation of the quantitation of percent G2/M and percent sub-G1 cells at the three dose regimes (5, 10, and 25 μM) at the noted hours. Results are representative of three experiments performed in triplicate.

ation of cells having hypodiploid DNA content reflects fragmented DNA indicating dying cells. The percent sub-G1 and G2/M population for the three doses (5, 10, and 25 μM) has been plotted in Figure 4D. It is evident from the line-graphical representation that at 25 μM for MCF-7 cells, the percent sub-G1 is 40%. However, at lower doses, the number of hypodiploid cells is lesser. We can clearly see differences at 5 and 10 μM CEFNA concentration in the extent of its deleterious effect on the cell cycle by the reduced percentage of sub-G1 cells. However, the apoptotic index seemed to saturate at a higher concentration of 25 μM.

3. Experimental

3.1. Chemistry

^{1}H NMR and ^{13}C NMR spectra were measured by 400 NMR spectrometer in a $CDCl_3$ solution and analyzed by INOVA. Proton NMR spectra were recorded at 400 MHz and were referenced with residual chloroform (7.27 ppm). Carbon NMR spectra were recorded at 100 MHz and were referenced with 77.27 ppm resonance of residual chloroform. Abbreviations for signal coupling are as follows: s, singlet; d, doublet; t, triplet; q, quartet; m, multiplet. Infrared spectra were recorded on sodium chloride discs on Mattson Genesis II FT-IR. High resolution mass spectra were collected on Thermo Finnigan LTQ-FT Hybrid mass spectrophotometer using 3-nitrobenzyl alcohol or with addition of LiI as a matrix. Melting points were determined using a Thomas-Hoover melting point apparatus and are uncorrected. All reactions were conducted with oven-dried (125 °C) reaction vessels in dry argon. All common reagents and solvents were obtained from Aldrich and were dried using 4 Å molecular sieves. The reactions were monitored by thin-layer chromatography (TLC) using silica gel 60 F254 (Merck) on precoated aluminum sheets. Flash chromatography was carried out on standard grade silica gel (230–400 mesh). HPLC purity data in two different solvent systems and peak attributions are provided in the supplementary information section.

3.1.1. (*R*)-5-((*S*)-4,5-dimethoxy-1,3-dihydroisobenzofuran-1-yl)-4-methoxy-6-methyl-5,6,7,8-tetrahydro-[1,3]-dioxolo[4,5-*g*]isoquinoline (2). To a solution of sodium borohydride (0.2 g, 5 mmol) in dry THF (20 ml) was added a solution of noscapine (1 g, 2.5 mmol) in boron trifluoride diethyrate drop wise at 0 °C. The mixture was stirred at 0 °C for 1 h and then refluxed for another 2 h. The reaction mixture was quenched with cold water, extracted with chloroform and dried (Na_2SO_4). Evaporation of the solvent afforded a crude product which was purified by flash column chromatography (ethyl acetate/hexane = 4:1) to afford the title compound **2**. Yield: 95%; ^{1}H NMR ($CDCl_3$, 400 MHz): δ 6.82 (d, 1H, J = 7.4 Hz), 6.56 (d, 1H, J = 7.4 Hz), 6.50 (s, 1H), 5.91 (s, 2H), 5.01 (dd, 1H, J = 11.6 Hz), 4.95 (dd, 1H, J = 11.6 Hz), 4.73 (s, 1H), 4.58 (s, 1H), 3.87 (s, 6H), 3.88 (s, 3H), 3.22–3.18 (m, 2H), 2.65 (s, 3H), 2.60–2.57 (m, 2H); ^{13}C NMR ($CDCl_3$, 100 MHz), δ 150.5, 148.5, 148.3, 148.0, 134.8, 133.5, 133.0, 131.1, 120.2, 118.5, 114.1, 104.8, 101.5, 97.2, 69.6, 65.4, 56.1, 56.0, 55.9, 52.7, 41.5, 31.8; HRMS (ESI): *m*/*z* Calcd for $C_{22}H_{26}NO_6$ (M+1), 400.44121; found: 400.4464 (M+1).

3.1.2. (*R*)-9-bromo-5-((*S*)-4,5-dimethoxy-1,3-dihydroisobenzofuran-1-yl)-4-methoxy-6-methyl-5,6,7,8-tetrahydro-[1,3]dioxolo[4,5-*g*]isoquinoline (3). To a flask containing the cyclic ether noscapine analog **2** (20 g, 48.8 mmol) was added a minimum amount of 48% hydrobromic acid solution (~40 ml) to dissolve or make a suspension of the reactant. To this reaction mixture was then added freshly prepared bromine water (~250 ml) drop wise until an orange precipitate appeared. The reaction mixture was stirred at room temperature for 1 h to attain completion, neutralized to pH 10 using ammonia solution to afford a solid precipitate. The solid precipitate was recrystallized with ethanol to afford the cyclic ether brominated noscapine analog **3**. Yield, 80%; mp 113–114 °C; IR: 2950 (m), 2852 (m), 1635 (w), 1616 (m), 1450 (s), 1267 (s), 1226 (s), 1078 (s), 1035 (s) cm^{-1}; ^{1}H NMR ($CDCl_3$, 400 MHz), δ 6.73 (d, 1H, J = 8 Hz), 6.11 (d, 1H, J = 8 Hz), 6.08 (s, 2H), 5.78 (s, 2H), 5.33 (dd, 1H, J = 12 Hz), 5.05 (dd, 1H, J = 12 Hz), 4.90 (s, 1H), 3.86 (s, 6H), 3.83 (s, 3H), 3.42–3.19 (m, 2H), 2.99 (s, 3H), 2.82–2.80 (m, 2H); ^{13}C NMR ($CDCl_3$, 100 MHz),

δ 151.8, 151.6, 149.7, 148.8, 136.3, 135.8, 132.9, 131.1, 120.9, 121.5, 114.4, 106.0, 101.2, 97.9, 69.3, 65.2, 56.9, 56.6, 56.0, 52.5, 41.3, 27.9; MS (FAB): *m*/*z* (relative abundance, %), 480 (100), 478 (100), 462 (8), 460 (8.3), 300 (18), 298 (19), 179 (12.5); MALDI: *m*/*z* 478.5 $(M)^+$, 480.5; ESI: parent ion mass, 480, 478; daughter ion masses (intensity, %), 462 (74), 460 (52.5), 447 (21), 445 (16.6), 431 (83.3), 429 (66.6), 300 (79), 298 (74.7), 193 (11), 191 (23.5), 179 (100); HRMS (ESI): *m*/*z* Calcd for $C_{22}H_{25}BrNO_6$ (M+1), 479.3345; found: 479.3329 (M+1).

3.1.3. (*R*)-5-((*S*)-4,5-dimethoxy-1,3-dihydroisobenzofuran-1-yl)-9-fluoro-4-methoxy-6-methyl-5,6,7,8-tetrahydro-[1,3]dioxolo[4,5-*g*]isoquinoline (CEFNA, 4). To a solution of cyclic ether brominated noscapine analog **3** (1 g, 2.5 mmol) in anhydrous THF (20 ml) was added an excess of Amberlyst-A 26 (fluorine, polymer-supported, 2.5 g, 10 mequiv of dry resin, the average capacity of the resin is 4 mequiv/g) and the reaction mixture was refluxed for 12 h. The resin was filtered off and the solvent removed to afford the crude product which was purified by flash column chromatography (ethyl acetate/hexane = 4:1) to afford (*R*)-5-((*S*)-4,5-dimethoxy-1,3-dihydroisobenzofuran-1-yl)-9-fluoro-4-methoxy-6-methyl-5,6,7,8-tetrahydro-[1,3]dioxolo[4,5-*g*]isoquinoline **(4)** as light brown crystals. The recovery of resin was achieved by washing with 1 N NaOH and then rinsing thoroughly with water until neutrality to afford hydroxy-form of resin. It was then stirred overnight with 1 N aqueous hydrofluoric acid (250 ml), washed with acetone, ether, and dried in a vacuum oven at 50 °C for 12 h to afford the regenerated Amberlyst-A 26 (fluorine, polymer-supported). Yield: 72%; mp 117.5–117.8 °C; ^{1}H NMR ($CDCl_3$, 400 MHz): δ 6.77 (d, 1H, J = 8.1 Hz), 6.32 (d, 1H, J = 8.1 Hz), 6.12 (s, 2H), 5.87 (s, 2H), 5.12 (dd, 1H, J = 11.4 Hz), 4.97 (dd, 1H, J = 11.4 Hz), 4.80 (s, 1H), 3.93 (s, 6H), 3.88 (s, 3H), 3.47–3.33 (m, 2H), 2.80 (s, 3H), 2.64–2.61 (m, 2H); ^{13}C NMR ($CDCl_3$, 100 MHz), δ 152.1, 151.5, 149.9, 148.7, 137.5, 135.2, 132.1, 131.7, 120.4, 121.8, 114.2, 106.5, 102.0, 98.0, 69.7, 66.7, 56.0, 56.8, 55.4, 52.6, 41.4, 28.2; HRMS (ESI): *m*/*z* Calcd for $C_{22}H_{25}FNO_6$ (M+1), 418.4354; found: 418.4219 (M+1).

The purity of compound **4** was determined using HPLC in two different solvent systems and the peak attributions were measured in Ultimate Plus, LC Packings, Dionex, using C_{18} column and a gradient starting from 100% A and 0% B to 0% A and 100% B over 25 min at a flow of 40 ml/min. The peak attributions are indicated as retention times in minutes. The retention time and corresponding purity are 18.04 and 97.5% using method 1 (solvent system: A, 0.1% formic acid and B, acetonitrile), whereas 18.06 and 97.0% using method 2 (solvent system: A, 0.1% formic acid and B, methanol), respectively.

4. Biology

4.1. Cell lines and chemicals

Cell culture reagents were obtained from Mediatech, Cellgro. MCF-7 and MCF-7/Adr cells were maintained in Dulbecco's modified Eagle's medium 1X (DMEM) with 4.5 g/L glucose and L-glutamine (Mediatech, Cellgro) supplemented with 10% fetal bovine serum (Invitrogen, Carlsbad, CA) and 1% penicillin/streptomycin (Mediatech, Cellgro). MDA-MB-231 cells were grown in RPMI-1640 medium supplemented with 10% fetal bovine serum and 1% penicillin/streptomycin.

4.1.1. In vitro cell proliferation assay

4.1.1.1. Sulforhodamine B assay. The cell proliferation assay was performed in 96-well plates as described previously.[12,24] Adherent cells were seeded in 96-well plates at a density of 5×10^3 cells per well. They were treated with increasing gradient concentrations of CEFNA the next day while in log-phase growth. After 72 h of drug treatment, cells were fixed with 50% trichloroacetic acid and stained with 0.4% sulforhodamine B dissolved in 1% acetic acid. Cells were then washed with 1% acetic acid to remove the unbound dye. The protein-bound dye was extracted with 10 mM Tris base to determine the optical density at 564-nm wavelength.

4.1.1.2. Cell viability by trypan blue-exclusion assay. The loss of membrane integrity in dead and dying cells allows the preferential uptake of labels like trypan blue. At the end of the incubation times with 25 μM CEFNA, MDA-MB-231 cells were pelleted and washed with PBS. Fifty microliters of well-suspended cells was mixed with 50 μl of 0.4% trypan blue in 1× PBS, pH 7.4, and incubated at room temperature for 5 min. Microscopic examination followed and blue-stained cells were considered non-viable.

4.1.1.3. DAPI staining. Cell morphology was evaluated by fluorescence microscopy following DAPI staining (Vectashield, Vector Labs, Inc., Burlingame, CA). MCF-7 cells were grown on poly-L-lysine-coated coverslips in six-well plates and were treated with 25 μM CEFNA for 72 h. After incubation, coverslips were fixed in cold methanol and washed with PBS, stained with DAPI, and mounted on slides. Images were captured using a BX60 microscope (Olympus, Tokyo, Japan) with an 8-bit camera (Dage-MTI, Michigan City, IN) and IP Lab software (Scanalytics, Fairfax, VA). Apoptotic cells were identified by features characteristic of apoptosis (e.g., nuclear condensation, formation of membrane blebs, and apoptotic bodies).

4.1.1.4. Immunofluorescence microscopy. Cells adhered to poly-L-lysine-coated coverslips were treated with CEFNA for 0, 1, 12, 24, 48, and 72 h. After treatment, cells were fixed with cold (−20 °C) methanol for 5 min and then washed with phosphate-buffered saline (PBS) for 5 min. Non-specific sites were blocked by incubating with 100 μl of 2% BSA in PBS at 37 °C for 15 min. A mouse monoclonal antibody against α-tubulin (DM1A, Sigma) was diluted 1:500 in 2% BSA/PBS (100 μl) and incubated with the coverslips for 2 h at 37 °C. Cells were then washed with 2% BSA/PBS for 10 min at room temperature before incubating with a 1:200 dilution of a fluorescein-isothiocyanate (FITC)-labeled goat anti-mouse IgG antibody (Jackson ImmunoResearch, Inc., West Grove, PA) at 37 °C for 1 h.

Coverslips were then rinsed with 2% BSA/PBS for 10 min and incubated with propidium iodide (0.5 μg/ml) for 15 min at room temperature before they were mounted with Aquamount (Lerner Laboratories, Pittsburgh, PA) containing 0.01% 1,4-diazobicyclo(2,2,2)octane (DABCO, Sigma). Cells were then examined using confocal microscopy for microtubule morphology and DNA fragmentation (at least 100 cells were examined per condition). Propidium iodide staining of the nuclei was used to visualize the multinucleated and micronucleated DNA in this study.

4.1.1.5. Cell-cycle analysis. The flow cytometric evaluation of the cell-cycle status was performed as described previously.[12] Briefly, 2×10^6 cells were centrifuged, washed twice with ice-cold PBS, and fixed in 70% ethanol. Tubes containing the cell pellets were stored at 4 °C for at least 24 h. Cells were then centrifuged at 1000*g* for 10 min and the supernatant was discarded. The pellets were washed twice with 5 ml of PBS and then stained with 0.5 ml propidium iodide (0.1% in 0.6% Triton X in PBS) and 0.5 ml RNase A (2 mg/ml) for 45 min in dark. Samples were then analyzed on a FACSCalibur flow cytometer (Beckman Coulter Inc., Fullerton, CA).

5. Conclusion

Summarizingly, we have provided a simple method for the regioselective fluorination of cyclic ether noscapine analog to yield the fluorinated product in high quantitative yields. Our results show that this novel analog inhibits proliferation of breast cancer cells including a drug-resistant variant much more potently than the parent compound, noscapine. Furthermore, the mechanism of cell death caused by CEFNA is preserved, in that, like noscapine, cell death is preceded by extensive mitotic arrest. Taken together, this novel analog indicates a great potential for further preclinical and clinical evaluation.

Acknowledgments

We are grateful to Dr. Wu and Dr. Fred Strobel of Department of Chemistry, Emory University for assistance with the NMR and High Resolution Mass spectrometry, respectively. We greatly acknowledge the superb technical assistance of Binfei Zhou. This work was supported by a NIH grant to HCJ.

References and notes

1. Dumontet, C.; Isaac, S.; Souquet, P. J.; et Bejui-Thivolet, F.; Pacheco, Y.; Peloux, N.; Frankfurter, A.; Luduena, R.; Perol, M. *Bull. Cancer* **2005**, *92*, E25.
2. Monzo, M.; Rosell, R.; Sanchezm, J. J.; Lee, J. S.; O'Brate, A.; Gonzalez-Larriba, J. L.; Alberola, V.; Lorenzo, J. C.; Nunez, L.; Ro, J. Y.; Martin, C. *J. Clin. Oncol.* **1999**, *17*, 1786.
3. Ranganathan, S.; Dexter, D. W.; Benetatos, C. A.; Chapman, A. E.; Tew, K. D.; Hudes, G. R. *Cancer Res.* **1996**, *56*, 2584.
4. Rowinsky, E. K. *Annu. Rev. Med.* **1997**, *48*, 353.
5. van Tellingen, O.; Sips, J. H.; Beijnen, J. H.; Bult, A.; Nooijen, W. J. *Anticancer Res.* **1992**, *12*, 1699.
6. Crown, J.; O'Leary, M. *Lancet* **2000**, *355*, 1176.
7. Ye, K.; Ke, Y.; Keshava, N.; Shanks, J.; Kapp, J. A.; Tekmal, R. R.; Petros, J.; Joshi, H. C. *Proc. Natl. Acad. Sci. U.S.A.* **1998**, *95*, 1601.
8. Aneja, R.; Zhou, J.; Vangapandu, S. N.; Zhou, B.; Chandra, R.; Joshi, H. C. *Blood* **2006**, *107*, 2486.
9. Aneja, R.; Vangapandu, S. N.; Lopus, M.; Viswesarappa, V. G.; Dhiman, N.; Verma, A.; Chandra, R.; Panda, D.; Joshi, H. C. *Biochem. Pharmacol.* **2006**, *12*, 28, [Epub ahead of print].
10. Aneja, R.; Lopus, M.; Zhou, J.; Vangapandu, S. N.; Ghaleb, A.; Yao, J.; Nettles, J. H.; Zhou, B.; Gupta, M.; Panda, D.; Chandra, R.; Joshi, H. C. *Cancer Res.* **2006**, 3782.
11. Aneja, R.; Vangapandu, S. N.; Lopus, M.; Chandra, R.; Panda, D.; Joshi, H. C. *Mol. Pharmacol.* **2006**, *69*, 1801.
12. Zhou, J.; Gupta, K.; Aggarwal, S.; Aneja, R.; Chandra, R.; Panda, D.; Joshi, H. C. *Mol. Pharmacol.* **2003**, *63*, 799.
13. Zhou, J.; Liu, M.; Aneja, R.; Chandra, R.; Joshi, H. C. *Biochem. Pharmacol.* **2004**, *68*, 2435.
14. Zhou, J.; Liu, M.; Luthra, R.; Jones, J.; Aneja, R.; Chandra, R.; Tekmal, R. R.; Joshi, H. C. *Cancer Chemother. Pharmacol.* **2005**, *55*, 461.
15. Checchi, P. M.; Nettles, J. H.; Zhou, J.; Snyder, J. P.; Joshi, H. C. *Trends Pharmacol. Sci.* **2003**, *24*, 361.
16. Joshi, H. C.; Zhou, J. *Drug News Perspect.* **2000**, *13*, 543.
17. Aggarwal, S.; Ghosh, N. N.; Aneja, R.; Joshi, H. C.; Chandra, R. *Helv. Chim. Acta* **2002**, *85*, 2458.
18. Dey, B. B.; Srinivasan, T. K. J. *Ind. Chem. Soc.* **1935**, *12*, 526.
19. Cainelli, G.; Manescalchi, F. *Synthesis* **1976**, 472.
20. Landen, J. W.; Lang, R.; McMahon, S. J.; Rusan, N. M.; Yvon, A. M.; Adams, A. W.; Sorcinelli, M. D.; Campbell, R.; Bonaccorsi, P.; Ansel, J. C.; Archer, D. R.; Wadsworth, P.; Armstrong, C. A.; Joshi, H. C. *Cancer Res.* **2002**, *62*, 4109.
21. Zhu, A.; Wang, X.; Guom, Z. *Nucl. Med. Biol.* **2001**, *28*, 735.
22. Lee, M.; Koh, W. S.; Han, S. S. *Cancer Lett.* **2003**, *193*, 57.
23. Zhou, J.; Yao, J.; Joshi, H. C. *J. Cell Sci.* **2002**, *115*, 3547.
24. Skehan, P.; Storeng, R.; Scudiero, D.; Monks, A.; McMahon, J.; Vistica, D.; Warren, J. T.; Bokesch, H.; Kenney, S.; Boyd, M. R. *J. Natl. Cancer Inst.* **1990**, *82*, 1107.